Inorg. Chem. **2007**, *46*, 10869–10876

DNA Binding and Topoisomerase II Inhibitory Activity of Water-Soluble Ruthenium(II) and Rhodium(III) Complexes

Sanjay Kumar Singh,[†] Shweta Joshi,[‡] Alok Ranjan Singh,[‡] Jitendra Kumar Saxena,[‡] and Daya Shankar Pandey*,[†]

Department of Chemistry, Faculty of Science, Banaras Hindu University, Varanasi -221 005 (U.P.), India, and Division of Biochemistry, Central Drug Research Institute, Chattar Manzil P.O. Box 173, Lucknow-226 001 (U.P.), India

Received May 8, 2007

Water-soluble piano-stool arene ruthenium complexes based on 1-(4-cyanophenyl)imidazole (CPI) and 4-cyanopyridine (CNPy) with the formulas $[(\eta^6\text{-arene})RuCl_2(L)]$ (L = CPI, η^6-arene = benzene (**1**), *p*-cymene (**2**), hexamethylbenzene (**3**); L = CNPy, η^6-arene = benzene (**4**), *p*-cymene (**5**), hexamethylbenzene (**6**)) have been prepared by our earlier methods. The molecular structure of $[(\eta^6\text{-}C_6Me_6)RuCl_2(CNPy)]$ (**6**) has been determined crystallographically. Analogous rhodium(III) complex $[(\eta^5\text{-}C_5Me_5)RhCl_2(CPI)]$ (**7**) has also been prepared and characterized. DNA interaction with the arene ruthenium complexes and the rhodium complex has been examined by spectroscopic and gel mobility shift assay; condensation of DNA and B→Z transition have also been described. Arene ruthenium(II) and EPh_3 (E = P, As)-containing arene ruthenium(II) complexes exhibited strong binding behavior, however, rhodium(III) complexes were found to be Topo II inhibitors with an inhibition percentage of 70% (**7**) and 30% (**7a**). Furthermore, arene ruthenium complexes containing polypyridyl ligands also act as mild Topo II inhibitors (10%, **3c** and 40%, **3d**) in contrast to their precursor complexes. Complexes **4**–**6** also show significant inhibition of β-hematin/hemozoin formation activity.

Introduction

Interaction of transition metal complexes with nucleobases/DNA has received considerable attention over the period of past couple of decades.[1] Although, the most significant metal-based anticancer drug, cisplatin, revolutionized cancer therapy, its toxicity leads to side effects, limiting the doses that can be administered, and is ineffective against certain types of cancer. This provides the impetus for the development of drugs based on other metals.[2] In this direction, efficacy of a number of nontransition and transition metals have been examined.[1,3−5] It has been established that ruthenium is the most attractive metal in this regard owing to its redox-accessible oxidation states, low toxicity, and ability to mimic iron binding in biological systems.[6] A number of ruthenium complexes show high *in vivo* and *in vitro* antitumor activity,

* To whom correspondence should be addressed. E-mail: dspbhu@bhu.ac.in. Phone: + 91 542 2307321.
[†] Banaras Hindu University.
[‡] Central Drug Research Institute.

(1) (a) Dale, L. D.; Tocher, J. H.; Dyson, T. M.; Edwards, D. I.; Tocher, D. A. *Anti-cancer Drug Des.* **1992**, *7*, 3. (b) Roitzsch, M.; Rother, I. B.; Willermann, M.; Erxleben, A.; Costisella, B.; Lippert, B. *Inorg. Chem.* **2002**, *41*, 5946. (c) Sullivan, S. T.; Ciccarese, A.; Fanizzi, F. P.; Marzilli, L. G. *Inorg. Chem.* **2000**, *39*, 836. (d) Suh, J. *Acc. Chem. Res.* **2003**, *36*, 562. (e) Ang, W. H.; Pilet, S.; Scopelliti, R.; Bussy, F.; Juillerat-Jeanneret, L.; Dyson, P. J. *J. Med. Chem.* **2005**, *48*, 8060. (f) Dyson, P. J.; Sava, G. *Dalton. Trans.* **2006**, 1929. (g) Sakai, K.; Ozawa, H.; Yamada, H.; Tusubomura, T.; Hara, M.; Higuchi, A.; Haga, M. *Dalton Trans.* **2006**, 3300. (h) Zhao, Y.; He, W.; Shi, P.; Zhu, J.; Qiu, J.; Qiu, L.; Lin, L.; Guo, Z. *Dalton Trans.* **2006**, 2617.

(2) (a) Pineto, H. M.; Schornagel, J. H. *Platinum and Other Metal Coordination Compounds in Cancer Chemotherapy*; Plenum: New York, 1996. (b) Rosenberg, B.; VanCamp, L.; Krigas, T. *Nature* **1965**, *205*, 698. (c) Fuertes, M. A.; Alonso, C.; Perez, J. M. *Chem. Rev.* **2003**, *103*, 645.

(3) (a) Metcalfe, C.; Thomas, J. A. *Chem. Soc. Rev.* **2003**, *32*, 215. (b) Erkkila, K. E.; Odom, D. T.; Barton, J. K. *Chem. Rev.* **1999**, *99*, 2777. (c) Clarke, M. J.; Zhu, F. C.; Frasca, D. R. *Chem. Rev.* **1999**, *99*, 2511. (d) Fish, R. H.; Jaouen, G. *Organometallics* **2003**, *22*, 2166. (e) Dorcier, A.; Ang, W. H.; Bolaño, S.; Gonsalvi, L.; Juillerat-Jeannerat, L.; Laurenczy, G.; Peruzzini, M.; Phillips, A. D.; Zanobini, F.; Dyson, P. J. *Organometallics* **2006**, *25*, 4090.

(4) (a) Lincoln, P.; Norden, B. *Chem. Commun.* **1996**, 2145. (b) Spillane, C. B.; Morgan, J. L.; Fletcher, N. C.; Collins, J. G.; Keene, F. R. *Dalton Trans.* **2006**, 3122. (c) Maheswari, P. U.; Rajendiran, V.; Stoeckli-Evans, H.; Palaniandavar, M. *Inorg. Chem.* **2006**, *45*, 37.

(5) (a) Sharma, S.; Chandra, M.; Pandey, D. S. *Eur. J. Inorg. Chem.* **2004**, 3555. (b) Singh, S. K.; Sharma, Chandra, M.; Pandey, D. S. *J. Organomet. Chem.* **2005**, *690*, 3105. (c) Sharma, S.; Singh, S. K.; Chandra, M.; Pandey, D. S. *J. Inorg. Bio. Chem.* **2005**, *99*, 458. (d) Chandra, M.; Sahay, A. N.; Pandey, D. S.; Tripathi, R. P.; Saxena, J. K.; Reddy, V. J. M.; Puerta, M. C.; Valerga, P. *J. Organomet. Chem.* **2004**, *689*, 2256.

10.1021/ic700885m CCC: $37.00
Published on Web 11/15/2007

and some of the ruthenium compounds, viz., NAMI-A [ImH] [*trans*-$RuCl_4$(DMSO)Im] and KP 1019 [ImH] [*trans*-$RuCl_4Im_2$], are of immense interest and are currently in clinical trials.[7] Among the coordination complexes, organometallic ruthenium complexes, especially η^6-arene ruthenium complexes, are being studied as potential anticancer agents. Excellent work of Sadler et al. and rich contributions from Dyson's research group and others on the anticancer activity of piano-stool arene ruthenium complexes have effectively highlighted the details and mechanistic aspects of interaction of arene ruthenium(II) complexes with DNA.[8] It has been shown that the extent of cytotoxicity of the arene ruthenium-based drugs can be monitored by using substituted arenes or arenes with extended π-systems, which provides a hydrophobic face for the complex and enhances biomolecular recognition. Substitution of the labile halogen ligands by a chelating ligand can help to control the stability and ligand exchange kinetics of these complexes.[2d,6a,b,8a,b]

DNA topoisomerases, which are intricately involved in maintaining the topographic structure of DNA transcription and mitosis, have been identified as an important biochemical target in cancer chemotherapy and microbial infections.[9] Also, DNA topoisomerase II (Topo II) of the filarial parasite *Setaria cervi* have been identified as a target for the development of antifilarial compounds. Recently, we have reported a variety of octahedral ruthenium(II) and analogous osmium(II) complexes based on polypyridyl and pyridylazine ligands with an aim to identify potential inhibitors of Topo II activity.[5a,d,10] We have shown that inhibition percentage in such systems largely depends on the nature of the complexes, ligands involved, and the presence of uncoordinated sites on the coordinated ligands. In this paper we report Topo II inhibitory activity of filarial parasite *Setaria cervi* by a variety of water-soluble piano-stool arene ruthenium complexes: [(η^6-arene)$RuCl_2$(L)], L = CPI, η^6-arene = benzene (**1**), *p*-cymene (**2**), hexamethylbenzene (**3**); L = CNPy, η^6-arene = benzene (**4**), *p*-cymene (**5**), hexamethylbenzene (**6**); related rhodium complex [(η^5-C_5Me_5)$RhCl_2$(CPI)] (**7**) and its derivatives imparting potential bridging ligands 1-(4-cyanophenyl)imidazole (CPI) and 4-cyanopyridine (CNPy) and its derivatives. We also describe herein heme polymerase inhibitory activity in malarial parasites by the complexes [(η^6-arene)$RuCl_2$(CNPy)].

Experimental Section

Materials and Methods. All the chemicals used were of analytical grade, and solvents were distilled and dried prior to their use following standard literature procedures.[11] Complexes **1**−**7**, **1a**−**7a**, **1b**−**3b**, and **3c**,**d** were prepared and purified by our earlier procedures.[12] Triply distilled deionized water was used for the preparation of various buffers. CT-DNA (calf thymus) and supercoiled pBR322 DNA was procured from Sigma Chemical Co., St. Louis, MO. Topoisomerase II from filarial parasite *Setaria cervi* was partially purified according to the method by Pandya et al.[13]

Crystal Structure Determination. Brown block-shaped single crystals of **6** with approximate dimensions of 0.35 × 0.30 × 0.30 mm were used for X-ray diffraction analyses. Intensity data were collected at 293(2) K on an Enraf-Nonius CAD4 (MACH 3) diffractometer using graphite monochromated Mo K_α radiation (λ = 0.71073). The structure was solved by direct methods and refined by Maxus-99 and SHELX-97.[14] Non-hydrogen atoms had anisotropically refined thermal parameters. All the hydrogen atoms were geometrically fixed and refined using a rigid model. Crystallographic data and selected bond parameters are recorded in Tables 1 and 2, respectively.

Absorption Titration and Emission Spectral Studies. Absorption titration studies were performed with a constant concentration of the complexes (30 μM) and a CT-DNA concentration varying between 0 and 17 μM in the spectral region 200−600 nm. Aqueous Tris buffer (5 mM Tris-HCl, 50 mM NaCl; 7.1 pH) was used for spectroscopic titrations. Emission intensity of the complexes in the absence and presence of CT-DNA (10 μM) was measured between 420 and 560 nm.

Gel Mobility Shift Assays. The enzymatic activity of topoisomerase II was monitored by relaxation of supercoiled pBR322 DNA.[13a,15] For the relaxation assay, the reaction mixture (20 μL) contained 50 mM Tris-HCl, pH 7.5, 50 mM KCl, 1 mM $MgCl_2$, 1 mM ATP, 0.1 mM EDTA, 0.5 mM DTT, 30 μg/mL BSA, and

(6) (a) Ang, W. H.; Dyson, P. J. *Eur. J. Inorg. Chem.* **2006**, *4003*. (b) Ang, W. H.; Scolaro, C.; Scopelliti, R.; Juillerat-Jeannerat, L.; Dyson, P. J. *Inorg. Chem.* **2006**, *45*, 9006. (c) Deubel, D. V.; Lau, J. K.-C. *Chem. Commun.* **2006**, 2451. (d) Romerosa, A.; Campos-Malpartida, T.; Lidrissi, C.; Saoud, M.; Serrano-Ruiz, M.; Peruzzini, M.; Garrido-Cárdenas, J. A.; Garcia-Maroto, F. *Inorg. Chem.* **2006**, *45*, 1289.

(7) (a) Sava, G.; Alessio, E.; Bergamo, A.; Mestroni, G. in *Topics in Biological Inorganic Chemistry*; Clarke, M. J.; Sadler, P. J., Eds., Springer-Verlag: Berlin, 1999; Vol. 1, p 143. (b) Bergamo, A.; Zorzet, S.; Gava, B.; Sorc, A.; Alessio, E.; Iengo, E.; Sava, G. *Anticancer Drugs* **2000**, *11*, 665.

(8) (a) Peacock, A. F. A.; Habtemariam, A.; Fernández, R.; Walland, V.; Fabbiani, F. P. A.; Parsons, S.; Aird, R. E.; Jodrell, D. I.; Sadler, P. J. *J. Am. Chem. Soc.* **2006**, *128*, 1739. (b) Yan, Y. K.; Melchart, M.; Habtemariam, A.; Sadler, P. J. *Chem. Commun.* **2005**, 4764. (c) Scolaro, C.; Bergamo, A.; Brescacin, L.; Delfino, R.; Cocchietto, M.; Laurenczy, G.; Geldbach, T. J.; Sava, G.; Dyson, P. J. *J. Med. Chem.* **2005**, *48*, 4161. (d) Aird, R. E.; Cummings, J.; Ritchie, A. A.; Muir, M.; Morris, R. E.; Chen, H.; Sadler, P. J.; Jodrell, D. I. *Br. J. Cancer* **2002**, *86*, 1652. (e) Wang, F.; Chen, H.; Parkinson, J. A.; Murdoch, P. del S.; Sadler, P. J. *Inorg. Chem.* **2002**, *41*, 4509. (f) Morris, R. E.; Aird, R. E.; Murdoch, P. del S.; Chen, H.; Cummings, J.; Hughes, N. D.; Parsons, S.; Parkin, A.; Boyd, G.; Jodrell, D. I.; Sadler, P. J. *J. Med. Chem.* **2001**, *44*, 3616.

(9) (a) Gopal, Y. N. V.; Konuru, N.; Kondapi, A. K. *Arch. Biochem. Biphys.* **2002**, *401*, 53. (b) Pyle, A. M.; Rehmann, J. P.; Meshoyrer, R.; Kumar, C. V.; Turro, N. J.; Barton, J. K. *J. Am. Chem. Soc.* **1989**, *111*, 3051. (c) Jenkins, Y.; Friedman, A. E.; Turro, N. J.; Barton, J. K. *Biochemistry* **1992**, *31*, 10809.

(10) Pandey, D. S.; Sahay, Sisodia, O. S.; Jha, N. K.; Sharma, P.; Klaus, H. E.; Cabrera, A. *J. Organomet. Chem.* **1999**, *592*, 278.

(11) Perrin, D. D.; Armango, W. L. F.; Perrin, D. R. *Purification of Laboratory Chemicals*; Pergamon: Oxford, U.K., 1986.

(12) (a) Singh, S. K.; Trivedi, M.; Chandra, M.; Sahay, A. N.; Pandey, D. S. *Inorg. Chem.* **2004**, *43*, 8600. (b) Gupta, D. K.; Sahay, A. N.; Pandey, D. S.; Jha, N. K.; Sharma, P.; Espinosa, G.; Cabrera, A.; Puerta, M. C.; Valerga, P. *J. Organomet. Chem.* **1998**, *568*, 13. (c) Singh, A.; Sahay, A. N.; Pandey, D. S.; Puerta, M. C.; Valerga, P. J. *Organomet. Chem.* **2000**, *605*, 74. (d) Pandey, D. S.; Sahay, A. N.; Agrawala, U. C. *Indian J. Chem.* **1996**, *35A*, 434. (e) Singh, S. K.; Trivedi, M.; Chandra, M.; Pandey, D. S. *J. Organomet. Chem.* **2005**, *690*, 647.

(13) (a) Pandya, U.; Saxena, J. K.; Kaul, S. M.; Murthy, P. K.; Chatterjee, R. K.; Tripathi, R. P.; Bhaduri, A. P.; Shukla, O. P. *Med. Sci. Res.* **1999**, *27*, 103. (b) Tripathi, R. P.; Rastogi, S. K.; Kundu, B.; Saxena, J. K.; Reddy, V. J. M.; Shrivastav, S.; Chandra, S.; Bhaduri, A. P. *Comb. Chem. Throughput Screening* **2001**, *4*, 237.

(14) (a) Mackay, S.; Dong, W.; Edwards, C.; Henderson, A.; Gilmox, C.; Stewart, N.; Shankland, K.; Donald, A. University of Glasgow, Scotland, 1999. (b) Sheldrick, G. M. SHELX-97: *Programme for the solution and refinement of crystal structures*; University of Göttingen: Germany, 1997.

(15) Burden, D. A.; Osheroff, N. *Biochim. Biophys. Acta* **1998**, *1400*, 139.

Table 1. Crystallographic Data for **6**

formula	$C_{18}H_{22}Cl_2N_2Ru$
M_r	438.35
space group	$P2_1/n$
crystal system	monoclinic
a/Å	9.067(2)
b/Å	12.4175(13)
c/Å	16.254(3)
α/deg	90
β/deg	102.691(18)
γ/deg	90
V/Å^3	1785.4(6)
Z	4
D_c/g cm^{-1}	1.631
F(000)	888
λ(Mo Kα)/Å	0.71073
μ/mm^{-1}	1.178
reflns collctd/unique (R_{int})	4245/3992 (0.0436)
$R(F^2)$ (obsd reflns)	$R_1 = 0.0617$, $wR_2 = 0.1708$
$R(F^2)$ (all reflns)	$R_1 = 0.1103$, $wR_2 = 0.2198$
GOF	1.112

Table 2. Selected Bond Lengths (Å), Bond Angles (Å), and Torsion Angles (deg) for **6**

Ru(1)−N(1)	2.136(6)
Ru(1)−C_{av}	2.208
Ru(1)−C_{ct}	1.682
Ru(1)−Cl(1)	2.422(2)
Ru(1)−Cl(2)	2.423(2)
C_{ring}−C_{ring}	1.430
C_{ring}−C_{Me}	1.507
N(1)−C(18)	1.340(10)
N(1)−C(13)	1.355(9)
N(2)−C(16)	1.148(11)
N(1)−Ru(1)−Cl(1)	85.46(17)
N(1)−Ru(1)−Cl(2)	85.82(17)
Cl(1)−Ru(1)−Cl(2)	88.72(9)
N(1)−C(13)−C(14)−C(15)	1.2(11)
C(1)−C(2)−C(3)−C(4)	−0.2(11)

enzyme protein. pBR322 supercoiled DNA (0.25 μg) was used as a substrate. The reaction mixture was incubated for 30 min at 37 °C and stopped by addition of 5 μL of loading buffer containing 0.25% bromophenol blue, 1 M sucrose, 1 mM EDTA, 0.5% SDS. Samples were applied on horizontal 1% agarose gels in 40 mM Tris-acetate buffer, pH 8.3, 1 mM EDTA, and run for 10 h at room temperature at 20 V. The gel was stained with ethidium bromide (0.5 μg/mL) and photographed in a GDS 7500 UVP (Ultra Violet Products, UK) transilluminator. One unit of topoisomerase activity is defined as the amount of enzyme required to relax 50% of the supercoiled DNA under the standard assay conditions.

DNA condensation was monitored by following the increase in the value of absorbance at 320 nm (A_{320}) against different complex/DNA ratios, according to the method of Barn and Marton.[16] The conformational transition of calf thymus CT-DNA in the presence of complexes was determined spectrophotometrically.[17] The UV absorbance ratio of A_{260}/A_{295} was monitored for B→Z DNA conformational change in the DNA helix.

Heme Polymerase Assay. Antimalarial activity of the complexes was studied by examining their respective inhibition percentage against β-hematin formation.[18] 1 mL amount of reaction mixture contained 100 μL of 1 M sodium phosphate buffer, 20 μL of hemin (1.2 mg/mL), and 25 μL of *P. yoelii* enzyme in triple distilled water. 20 μg amount of the complex was added to the reaction mixture and incubated for 16 h at 37 °C in an incubator shaker at a speed of 174 rpm. After incubation, the reaction mixture was centrifuged at 10 000 rpm for 15 min, and the pellets obtained were washed three times with 10 mL of buffer containing 0.1 M Tris-Cl buffer, pH 7.5, and 2.5% SDS and then by buffer 2 (0.1 M sodium bicarbonate buffer, pH 9.2, and 2.5% SDS) followed by distilled water. Semidried pellets were suspended in 50 μL of 2 N NaOH, and the volume was adjusted to 1.0 mL with distilled water. Optical density was measured at 400 nm, and percent inhibition was calculated using the formula: % inhibition = {(1 − O.D. control)/O.D. experimental} × 100.

Results and Discussion

Synthesis and Structure. Chloro-bridged arene-capped ruthenium(II) complexes [(η^6-arene)$RuCl_2$(L)] (L = CPI; η^6-arene = benzene (**1**), *p*-cymene (**2**), hexamethylbenzene (**3**); L = CNPy; η^6-arene = benzene (**4**), *p*-cymene (**5**), hexamethylbenzene (**6**)) and the analogous rhodium(III) complex [(η^5-C_5Me_5)$RhCl_2$(CPI)] (**7**) were prepared by direct reaction of the chloro-bridged complexes [{(η^6-arene)Ru(μ-Cl)}$_2$] and [{(η^5-C_5Me_5)Rh(Cl)(μ-Cl)}$_2$], respectively, with CPI/CNPy in dichloromethane following our earlier procedures (Scheme 1 and 2).[12]

Substitution of one of the chlorides by EPh_3 (E = P, As, or Sb) in complexes **1**−**7** forced the prochiral metal center to a chiral center, leading to four different coordinated ligands: [(η^6-arene)RuCl(L)(CPI)]$^+$ (L = PPh_3, η^6-arene = benzene (**1a**), *p*-cymene (**2a**), hexamethylbenzene (**3a**); L = $AsPh_3$, η^6-arene = benzene (**1b**), *p*-cymene (**2b**), hexamethylbenzene (**3b**)); [(η^6-arene)RuCl(L)(CNPy)]$^+$ (L = PPh_3; η^6-arene = benzene (**4a**), *p*-cymene (**5a**), hexamethylbenzene (**6a**)); [(η^5-C_5Me_5)Rh(Cl)(PPh_3)(CPI)]$^+$ (**7a**). Substituting both chlorides with a bis-chelating ligand like 2,2′-bipyridine (bpy) or 1,10-phenanthroline (phen) from [(η^6-C_6Me_6)$RuCl_2$(CPI)] (**3a**) resulted in the complexes [(η^6-C_6Me_6)Ru(N−N)(CPI)]$^{2+}$ (N−N = bpy (**3c**) and phen (**3d**)).

Single-crystal X-ray structures of some of the complexes (**1a**, **2**, **2a**, **3**, **5**, and **5a**) have already been reported by us.[12] Suitable single crystals for [(η^6-C_6Me_6)$RuCl_2$(CNPy)] (**6**) were obtained from dichloromethane/diethyl ether by diffusion technique. The perspective view of the complex is shown in Figure 1, and crystallographic data and selected bond parameters are reported in the Tables 1 and 2, respectively.

In the asymmetric molecular unit of **6**, the metal center adopts a piano-stool geometry, coordinated to one η^6-C_6Me_6 as the top of the stool with three coordination sites occupied by two chloro and one CNPy ligand. The overall geometry of **6** is analogous to the structures of other complexes of this series.[12a,b] The average C−C distance in the hexamethylbenzene ring is 1.430 Å, ruthenium to carbon distances are almost equal with an average Ru−C distance of 2.208 Å [range 2.196−2.227 Å], and the ruthenium center is displaced by 1.682 Å from the centroid of the hexamethylbenzene ring.[12a−c,19] The Ru−Cl bond distance and Cl−Ru−Cl angles are normal and comparable to those reported in other related systems.[12,20] The ruthenium to

(16) Basu, H. S.; Marton, L. J. *Biochem. J.* **1987**, *244*, 243.
(17) Pohl, E. M.; Jovin, T. M. *J. Mol. Biol.* **1972**, *67*, 375.
(18) Pandey, A. V.; Singh, N.; Takevani, B. L.; Puri, S. K.; Chauhan, V. S. *J. Pharm. Biomed. Anal.* **1999**, *20*, 203.
(19) (a) Campagna, S.; Denti, G.; Derosa, G.; Sabatino, L.; Ciano, M.; Balzani, V. *Inorg. Chem.* **1989**, *28*, 2565. (c) Murphy, W. R.; Brewer, K. J.; Gettliffe, G.; Peterson, J. D. *Inorg. Chem.* **1989**, *28*, 81.

Scheme 1. Complexes of RACPI and RHOCPI Series

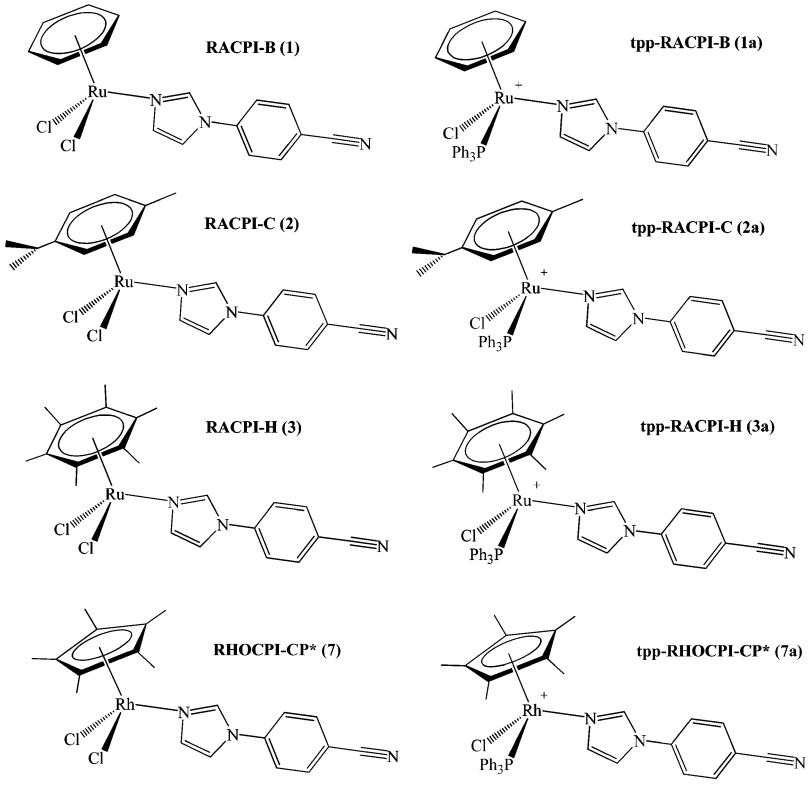

Scheme 2. Complexes of RAC Series

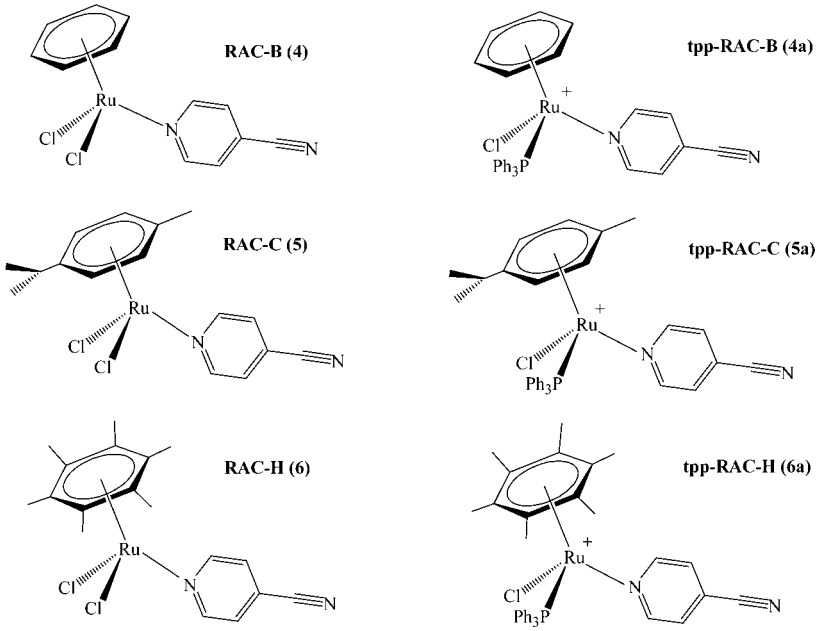

pyridyl nitrogen distance is 2.136(6) Å which is comparable to the closely related Ru(II) complexes $[(\eta^6\text{-}C_{10}H_{14})RuCl_2(CNPy)]$ (**5**) and $[(\eta^3{:}\eta^3\text{-}C_{10}H_{14})RuCl_2(CNPy)]$.[12b,c,21] The CN bond length of the pendent nitrile is 1.148(11) Å and is consistent with other reports.[12,21]

Crystal packing in **6** revealed the presence of face to face stacking interactions of the hexamethylbenzene rings with a centriod to centroid distance of 3.985(6) Å.[22] Both coordinated chloro groups are involved in various intermolecular

(20) (a) Davenport, A. J.; Davies, D. L.; Fawcett, J.; Garratt, S. A.; Russell, D. R. *J. Chem. Soc., Dalton Trans.* **2000**, 4432. (b) Hayashida, T.; Nagashima, H. *Organometallics* **2002**, *21*, 3884. (c) Nishiyama, H.; Konno, M.; Aoki, K. *Organometallics* **2002**, *21*, 2536. (d) Allardyce, C. S.; Dyson, P. J.; Ellis, D. J.; Heath, S. L. *Chem. Commun.* **2001**, 1396. (e) Frodl, A.; Herebian, D.; Sheldrick, W. S. *J. Chem. Soc., Dalton Trans* **2002**, 3664. (f) Chen, H. M.; Parkinson, J. A.; Parsons, S.; Coxall, R. A.; Gould, R. O.; Sadler, P. J. *J. Am. Chem. Soc.* **2002**, *124*, 3064.

(21) (a) Steed, J. W.; Tocher, D. A. *Inorg. Chim. Acta* **1991**, *189*, 135. (b) Brunner, H.; Oeschey, R.; Nuber, B. *J. Chem. Soc., Dalton Trans.* **1996**, 1499. (c) Sahay, A. N.; Pandey, D. S.; Walawalkar, M. G. *J. Organomet. Chem.* **2000**, *613*, 250.

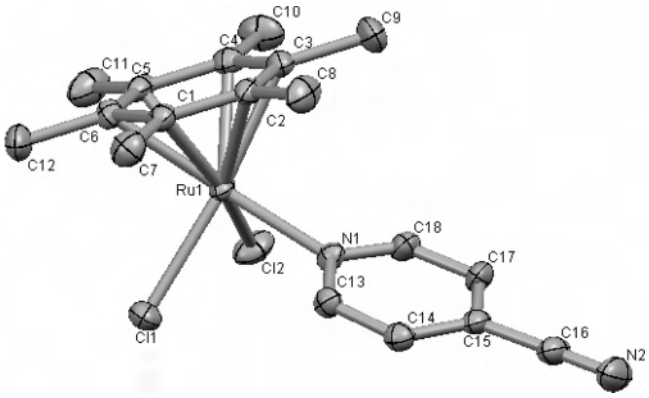

Figure 1. Solid-state molecular view for **6**.

C−H···Cl interactions with the methyl (C8−H8c···Cl2 *d* 2.944 Å, *D* 3.801 Å, *θ* 149.30°) and pyridyl (C17−H17···Cl1 *d* 2.930 Å, *D* 3.534 Å, *θ* 123.90°) hydrogen; however, no distinguished motif has been observed. The pendent nitrile is involved in a bifurcated C−H···N interaction with the methyl hydrogen of hexamethylbenzene (C7−H7a···N2 *d* 2.624 Å, *D* 3.551 Å, *θ* 162.27° and C8−H8c···N2 *d* 2.646 Å, *D* 3.557 Å, *θ* 158.10°).

DNA Interaction Studies. Spectroscopic Studies. Absorption titration studies performed on RACPI-B (**1**), RACPI-C (**2**), and RACPI-H (**3**) with calf thymus DNA (CT-DNA) demonstrated significant interaction between the complexes and nucleic acid. Titration of a solution of the complexes (30 μM) with CT-DNA (0−17 μM) shows a pronounced hypochromism (20% **1**; 39% **2**, and 29% **3**) at respective metal to ligand charge transfer (MLCT) bands; however, no significant bathochromic shifts have been observed. The observed hyprochromicity is expected to be associated with the interaction of the complexes with the DNA helix.[4,23] Absorption spectra were measured after equilibration, and the intrinsic binding constants were determined by monitoring the decay in absorbance with increasing concentration of CT-DNA. The intrinsic binding constant 'K_b' and binding site size '*s*' for **1** (6.37×10^5 M^{-1}, K_b; 0.10, *s*), **2** (2.15×10^5 M^{-1}, K_b; 0.11, *s*), and **3** (1.97×10^5 M^{-1}, K_b; 0.12, *s*) were determined by using the Bard and Thorp model for noncooperative and nonspecific binding, under identical conditions.[24] The observed binding constants for these complexes are consistent with other reports.[25] Interestingly, interaction of the complexes with the DNA helix is tuned by the possible steric hindrance imposed by the coordinated arene as inferred by the high K_b value for RACPI-B (**1**) (Figure 2).

The complexes **1**, **2**, and **3** show moderately strong emissions when excited at the respective MLCT band (**1**, λ_{em} 450 nm (λ_{ex} 400 nm); **2**, λ_{em} 462 nm (λ_{ex} 407 nm); **3**, λ_{em} 475 nm (λ_{ex} 412 nm). Interestingly, an increase in the emission intensity is observed for these complexes with CT-DNA under the conditions depicted in Figure 3. The observed enhancement could be correlated to the hindrance in the nonradiative deactivation process of the excited states because of possible interaction of the complexes with CT-DNA.[1f,5b,c] The initial evidence by spectral studies for interaction of the complex with nucleic acid is further strengthened by electrophoretic mobility studies of the plasmid DNA on agarose gel.

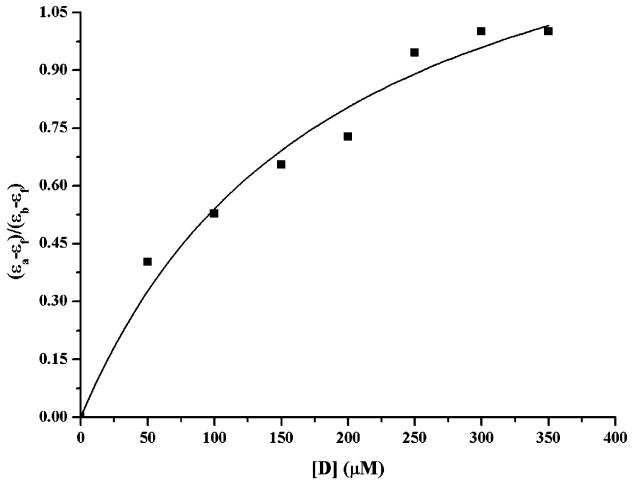

Figure 2. Absorption spectral plot of $(\epsilon_a - \epsilon_f)/(\epsilon_b - \epsilon_f)$ vs [DNA] for RACPI-B (**1**). The best fit line, superimposed on the data, $K_b = 6.37 \times 10^5$ M^{-1} ($s = 0.10$).

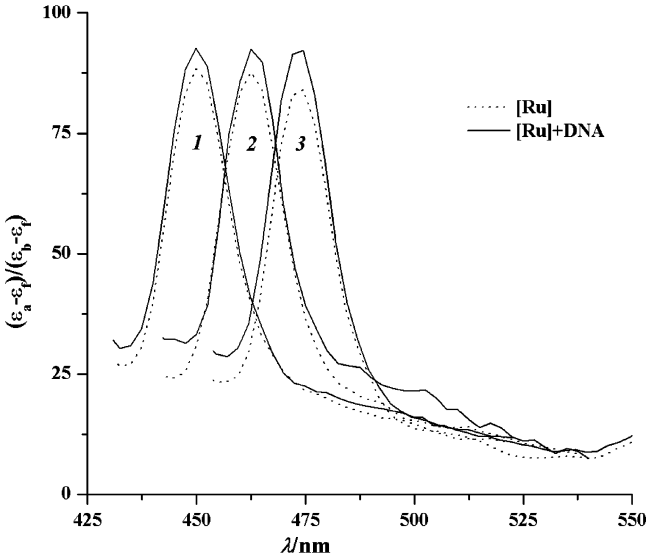

Figure 3. Emission spectra of **1**, **2**, and **3** in the absence and presence of CT-DNA (10 μM).

DNA Mobility Shift Assays. Change in the electrophoretic mobility of plasmid DNA on agarose gel is commonly taken as evidence for direct DNA−metal interactions. Alteration of the DNA structure causes retardation in the migration of

(22) (a) Desiraju, G. R.; Steiner, T. *The weak hydrogen bond in structural chemistry and biology*; Oxford University Press: Oxford, 1999. (b) Scaccianoce, L.; Braga, D.; Calhorda, M. J.; Grepioni, F.; Johnson, B. F. G. *Organometallics* **2000**, *19*, 790.

(23) (a) Fair, R. B.; Teng, E. S.; Kirkland, S. L.; Murphy, C. J. *Inorg. Chem.* **1998**, *37*, 139. (b) Ambroise, A.; Maiya, B. G. *Inorg. Chem.* **2000**, *39*, 4256.

(24) (a) Carter, M. T.; Rodriguez, M.; Bard, A. J. *J. Am. Chem. Soc.* **1989**, *111*, 8901. (b) Smith, S. R.; Neyhart, G. A.; Kalsbeck, W. A.; Thorp, H. H. *New J. Chem.* **1994**, *18*, 397.

(25) (a) Hiort, C.; Lincoln, P.; Norden, B. *J. Am. Chem. Soc.* **1993**, *115*, 3448. (b) Liu, J.-G., Zhang, Q.-L., Shi, X.-F., Ji, L.-N. *Inorg. Chem.* **2001**, *40*, 5045. (c) Neyhart, G. A.; Grover, N.; Smith, S. R.; Kalsbeck, W. A.; Fairley, T. A.; Cory, M.; Thorp, H. H. *J. Am. Chem. Soc.* **1993**, *115*, 4423.

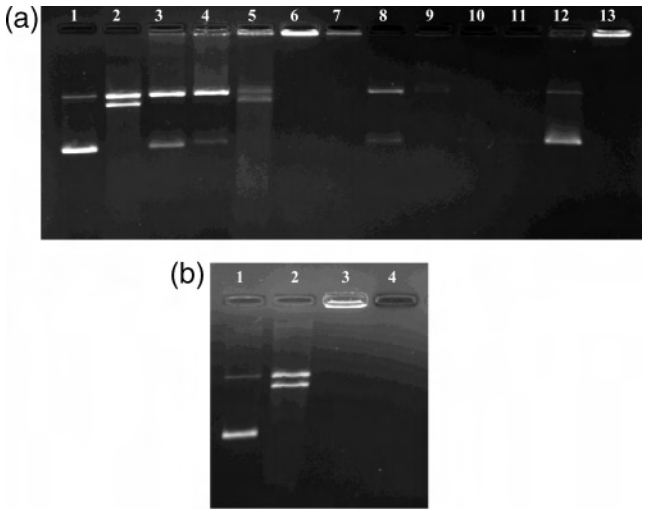

Figure 4. (a) Gel mobility shift assay of *S. cervi* topoisomerase II by complexes **3**, **1a**−**3a**, **1b**−**3b**, **3c**, **3d**, **7**, **and 7a** (40 μg). Lane 1: pBR322 (0.25μg) alone; lane 2: pBR322 + *S. cervi* Topo II; lane 3: **3d**; lane 4: **3c**; lane 5: **3b**; lane 6: **1b**; lane 7: **2b**; lane 8: **7a**; lane 9: **3a**; lane 10: **1a**; lane 11: **2a**; lane 12: **7**; lane 13: **3**. (b) Gel mobility shift assay of *S. cervi* topoisomerase II by complexes **1** and **2** (40 μg). Lane 1: pBR322 (0.25μg) alone; lane 2: pBR322 + *S. cervi* Topo II; lane 3: **1**; lane 4: **2**.

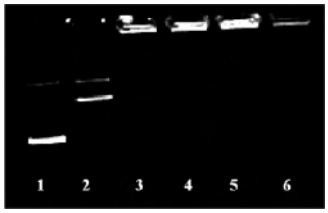

Figure 5. Gel mobility shift assay of *S. cervi* topoisomerase II by complexes **4**−**6** and **6a** (20 μg). Lane 1: pBR322 (0.25 μg) alone; lane 2: pBR322 + *S. cervi* Topo II; lane 3: **4**; lane 4: **5**; lane 5: **7** and lane 6: **5a**.

supercoiled DNA and a slight increase in the mobility of open circular DNA to a point where both forms comigrate. Interaction of the complexes with DNA Topo II was examined by studying the enzyme-mediated supercoiled pBR322 relaxation.[13,15] The noncovalent interaction of protein with DNA is the key step in the topoisomerase II catalytic cycle. Under physiological conditions, DNA replication, repair, and transcription processes are significantly controlled by Topo II.[26] Anti-Topo II agents control the Topo II activity either by trapping the Topo II−DNA complex or acting as Topo II inhibitors.[8f] Gel electrophoresis shows that arene-capped ruthenium-based RACPI (**1**−**3**) (Figure 4) and RAC (**4**−**6**) (Figure 5-7) complexes display different modes of interaction with Topo II of *S. cervi* than that of rhodium-centered systems RHOCPI (**7**) (Figure 4a). As observed by the upshift of bound DNA to the gel origin, complexes **1**−**3** and **1b**−**3b** greatly promoted the Topo II−DNA binding, while related phosphine-containing complexes **1a**−**3a** also promoted the above activity but to a lower extent. The observed complex formation with the RACPI and RAC series of complexes indicated that these complexes bind to the Topo II−DNA complex, or DNA, or the enzyme. However, closely related complexes, where both labile chloro groups are replaced by bpy (**3c**) and phen (**3d**), effected relaxation of

(26) Wang, J. C. *J. Biol. Chem.* **1991**, *266*, 6659.

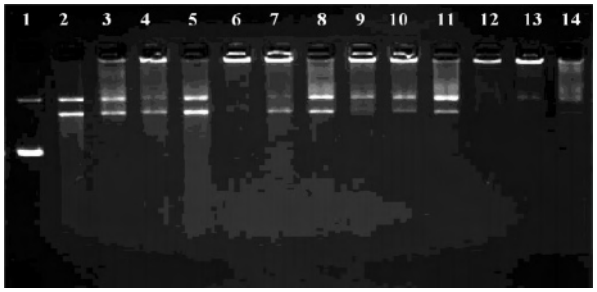

Figure 6. Gel mobility shift assay of *S. cervi* topoisomerase II by complexes **4**−**6** and **5a** (20 μg, lane 3, 6, 9, and 12; 10 μg, lane 4, 7, 10, and 13; 5 μg, lane 5, 8, 11, and 14). Lane 1: pBR322 (0.25 μg) alone; lane 2: pBR322 + *S. cervi* Topo II; lane 3−5: **4**; lane 6−8: **5**; lane 9−11: **6**, and lane 12−14: **5a**.

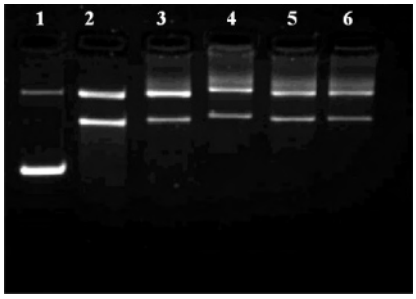

Figure 7. Gel mobility shift assay of *S. cervi* topoisomerase II by complexes **4**−**6** and **5a** (0.2 μg). Lane 1: pBR322 (0.25 μg) alone; lane 2: pBR322 + *S. cervi* Topo II; lane 3: **4**; lane 4: **5**; lane 5: **6**, and lane 6: **5a**.

the supercoiled DNA, with an inhibition percentage of 10% and 40%, respectively. Further, rhodium complexes RHOCPI (**7**, **7a**) induce relaxation of supercoiled DNA, displaying a significant inhibitory action of 70% for **7**, which was followed by its phosphine analogue (∼30% inhibition, **7a**), where the bulky PPh_3 destabilizes interaction with the DNA strand. These results are consistent with other PPh_3 containing systems, as the hydrophobic PPh_3 ligand enhances poor selectivity of the ruthenium based drugs, possibly because of increased drug uptake.[6a,c,8c,27]

The gel mobility assay of the 4-cyanopyridine complexes, RAC (**4**−**6**), also shows behavior analogous to that for the closely related RACPI complexes. Complexes **4**−**6** and **5a** exhibited strong complex formation at a concentration of 40 and 20 μg per reaction test with DNA topoisomerase of the filarial parasite (Figure 5). The effect of these complexes at 10, 5, 2 μg were also measured (Figures 6 and 7). It was found that at these concentrations also showed complex formation as indicated by presence of DNA in the well. Further, reducing the concentration to 0.2 μg led to a decrease in the complex intensity. Chart 1 shows the comparative Topo II inhibition percentage in descending order.

The aromatic group (η^5/η^6-arene) has significant effect on the drug uptake and *in vitro* activity, however, replacement of the aromatic group by another low sterically demanding

(27) (a) Serli, B.; Zangrando, E.; Gianferrara, T.; Scolaro, C.; Dyson, P. J.; Bergamo, A.; Alessio, E. *Eur. J. Inorg. Chem.* **2005**, 3423. (b) Phillips, A. D; Gonsalvi, L.; Romerosa, A.; Vizza, F.; Peruzzini, M. *Coord. Chem. Rev.* **2004**, *248*, 955. (c) McCaffrey, L. J.; Henderson, W.; Nicholson, B. K.; Mackay, J. E.; Dinger, M. B. *Dalton Trans.* **1997**, 2577.

Chart 1

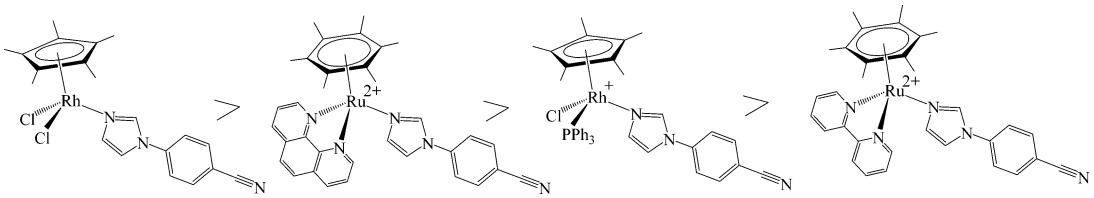

capping ligand influences only slightly the overall drug activity.[8c] Further, the control experiments of the complexes with DNA have been carried out in the absence of topoisomerase II. A concentration-dependent interaction has been observed, as these complexes are found to be poorly interactive or noninteractive with DNA in the absence of Topo II; however, they inhibited the DNA topoisomerase activity as measured by a significant conversion of supercoiled DNA to relaxed form DNA (see Supporting Information Figure S1−S6). These complexes seem to inhibit the first step of the DNA topoisomerase reaction, i.e., by inhibiting the binding of enzyme with the substrate or trapping the Topo II−DNA complex. Previously, strong topoisomerase inhibitory activity by arene-capped-ruthenium complexes was demonstrated as measured by formation of the cleavage complex or cross-linking with topoisomerase.[9]

The anomalous morphology of Z-DNA and its involvement in gene expression and recombination has attracted a great deal of attention from the scientific community on B−Z transitions. The B→Z form conversion in the presence of the complexes under study was followed spectrophotometrically by UV-absorption ratio of A_{260}/A_{295}. Dichloro ruthenium(II) arene and the related rhodium(III) complex showed enhancement in the ratio from 1.758 for free DNA to 4.696 (**1**), 7.603 (**3**), and 6.406 (**7**). A similar observation was made for the complexes of RAC series (3.115, 4.542, 5.176 (**4**−**6**), and 3.149 (**5a**)). Observed alterations in the UV absorbance ratio imply that the DNA helix shows B−Z conformational changes. Also such changes are found to be sterically controlled by the substituted arene on the metal center. It was observed that the complexes with highly substituted arene **3** (η^6-C_6Me_6), **6** (η^6-C_6Me_6), and **7** (η^5-C_5Me_5) have the highest value for the A_{260}/A_{295} ratio. Further, condensation of the CT-DNA induced by complexes was monitored spectroscopically by increase in the absorption value at 320 nm.[16] Negatively charged phosphate groups in DNA are the prime targets for the interaction of polyamines by electrostatic forces. Condensation is a function of charges and nucleotide sequence as well on specific macromolecular size and organization. In bacteria, DNA is packaged by nonhistone proteins, polyamines, and RNA. The condensation of DNA occurs when 80−90% of its negative charge is neutralized by multivalent and univalent counterions. Higher concentrations of polyamines cause condensation of DNA because most of the negative charges present on DNA are from electrostatic interaction. Further, the intra- and interchain interaction is also important in the condensation of DNA.[28,29]

Ruthenium(II) arene complexes containing 4-cyanopyridine (RAC) (**4**−**6**) also showed inhibitory effect on heme polymerization activity in presence of *P. yoelii* lysate. The heme polymerization activity was measured by β-hematin formation.[18] The complex **5a** showed 92.3% inhibition of heme polymerase activity, while complexes **4**−**6** cause 40.0, 52.4, 42.4% inhibition, respectively. The observed result could be attributed to the presence of PPh_3 in **5a** and are consistent with other systems containing PPh_3.[6a,c,8c,27]

Conclusions

The present work describes DNA binding behavior of a series of water-soluble *piano-stool* arene ruthenium and related rhodium complexes including 1-(4-cyanophenyl)-imidazole (CPI) and 4-cyanopyridine (CNPy) [(η^6-arene)-$RuCl_2$(L)] (L = CPI, η^6-arene = benzene (**1**), *p*-cymene (**2**), hexamethylbenzene (**3**); L = CNPy, η^6-arene = benzene (**4**), *p*-cymene (**5**), hexamethylbenzene (**6**)) and the analogous rhodium(III) complexes [(η^5-C_5Me_5)$RhCl_2$(CPI)] (**7**) and their derivatives. Complexes under study displayed interesting activity against DNA−Topo II interaction, which was measured by spectroscopic techniques and gel mobility shift assay. Ruthenium arene-centered complexes (RACPI **1**−**3** and RAC **4**−**6**) are found to be potential DNA binding agents, in contrast to the analogous rhodium(III) complexes which are active Topo II inhibitors. Further, the arene ruthenium complexes with coordinated polypyridyl ligands also act as Topo II inhibitors in contrast to its precursor complex **3**. Apart from the activity against DNA−Topo II interaction, RAC complexes also showed heme polymerization inhibitory activity. Complex **5a** exhibited 92.3% inhibition of heme polymerization activity.

Acknowledgment. We thank Department of Science and Technology, New Delhi, India, for financial assistance through the scheme SP/S1/F04/2000 and the Council of Scientific and Industrial Research, New Delhi, for the award of a Senior Research Fellowship to S.K.S. (9/13(97)/2006-EMR-I). We are also thankful to the Head, Department of Chemistry, Banaras Hindu University, Varanasi (U.P.), for extending facilities, and SAIF, Central Drug Research Institute, Lucknow (U.P.), India, for providing analytical and spectral data and Prof. P. Mathur, In-charge, National Single-

(28) Thomas, T. J.; Messner, R. P. *J. Mol. Biol.* **1988**, *201*, 463.
(29) (a) Clarke, M. J.; Zhu, F.; Frasca, D. R. *Chem. Rev.* **1999**, *99*, 2511. (b) McNae, I. W.; Fishburne, K.; Mabtemariam, A.; Hunter, T. M.; Melchart, M.; Wang, F.; Walkinshaw, M. D.; Sadler, P. J. *Chem. Commun.* **2004**, 1786. (c) Chen, H.; Parkinson, J. A.; Morris, R. E.; Sadler, P. J. *J. Am. Chem. Soc.* **2003**, *125*, 173.

crystal X− Ray Facility, Indian Institute of Technology, New Delhi, for single-crystal X-ray data.

Supporting Information Available: Crystallographic data of the complex **6** is available in CIF format. Details for the control experiments for the complexes (10 μg and 1 μg) **1**−**7**, **1a-3a**, **5a**, and **7a** with pBR322 DNA in the absence (Figure S1−S4) and presence (Figure S5−S6) of topoisomerase II. This material is available free of charge via the Internet at http://pubs.acs.org.

IC700885M